Supplementary material for: Jena Soil Model: a microbial soil organic carbon model integrated with nitrogen and phosphorus processes

Lin Yu[1], Bernhard Ahrens[1], Thomas Wutzler[1], Marion Schrumpf[1,2], Sönke Zaehle[1,2]
[1]Max Planck Institute for Biogeochemistry, Hans-Knöll Str. 10, 07745 Jena, Germany
[2]International Max Planck Research School (IMPRS) for Global Biogeochemical Cycles, Jena, Germany

Correspondence: Lin Yu (lyu@bgc-jena.mpg.de)

This appendix includes a detailed description of the model with equations and tables of parameter values.

S1 The SOM cycle

The model represents different soil organic pools (woody (wl), polymeric ($poly$), and soluable (sol) litter, as well as dissolved organic matter (DOM, dom), microbial biomass (mic), microbial residue (res), mineral-associated DOM ($aDom$), and mineral-associated microbial residue ($aRes$)), and the dynamics of them ($X =$ C, N, P, ^{13}C, ^{14}C, ^{15}N) are described in general as:

$$\frac{\partial}{\partial t}X_{wl} = \sum(f_{vp\to wl}F_{L_{vp}}) - \frac{X_{wl}}{\tau_{wl}} - \frac{\partial}{\partial z}(D_b\frac{\partial X_{wl}}{\partial z}) - \frac{\partial(\omega \cdot X_{wl_{sl>1}})}{\partial z} \tag{S1a}$$

$$\frac{\partial}{\partial t}X_{sol} = \sum(f_{vp\to sol}F_{L_{vp}}) - \frac{X_{sol}}{\tau_{sol}} - \frac{\partial}{\partial z}(D_b\frac{\partial X_{sol}}{\partial z}) - \frac{\partial(\omega \cdot X_{sol})}{\partial z} \tag{S1b}$$

$$\begin{aligned}\frac{\partial}{\partial t}X_{poly} = &\sum(f_{vp\to poly}F_{L_{vp}}) + \eta_{wl\to poly}\frac{X_{wl}}{\tau_{wl}} - F^{depoly}_{poly\to dom}\\ &- \frac{\partial}{\partial z}(D_b\frac{\partial X_{poly}}{\partial z}) - \frac{\partial(\omega \cdot X_{poly})}{\partial z}\end{aligned} \tag{S1c}$$

$$\begin{aligned}\frac{\partial}{\partial t}X_{dom} = &\eta_{sol\to dom}\frac{X_{sol}}{\tau_{sol}} + F^{depoly}_{poly\to dom} + F^{depoly}_{res\to dom} - F^{sorp}_{dom\to aDom}\\ &- F^{upt}_{dom\to mic} + \eta_{mic\to dom}\frac{X_{mic}}{\tau_{mic}} + \sigma_{recycle}\\ &- \frac{\partial v_{dom}dom}{\partial z} - \frac{\partial}{\partial z}(D_b\frac{\partial X_{dom}}{\partial z}) - \frac{\partial(\omega \cdot X_{dom})}{\partial z}\end{aligned} \tag{S1d}$$

$$\begin{aligned}\frac{\partial}{\partial t}X_{mic} = &F^{growth}_{mic} - \eta_{mic\to dom}\frac{X_{mic}}{\tau_{mic}} + \Phi_{immobilisation}\\ &- \frac{\partial}{\partial z}(D_b\frac{\partial X_{mic}}{\partial z}) - \frac{\partial(\omega \cdot X_{mic})}{\partial z}\end{aligned} \tag{S1e}$$

$$\begin{aligned}\frac{\partial}{\partial t}X_{res} = &\eta_{mic\to res}\frac{X_{mic}}{\tau_{mic}} - F^{depoly}_{res\to dom} - F^{sorp}_{res\to aRes} - \sigma_{recycle}\\ &- \frac{\partial}{\partial z}(D_b\frac{\partial X_{res}}{\partial z}) - \frac{\partial(\omega \cdot X_{res})}{\partial z}\end{aligned} \tag{S1f}$$

$$\frac{\partial}{\partial t}X_{aDom} = F^{sorp}_{res\to aRes} - \frac{\partial}{\partial z}(D_b\frac{\partial X_{aDom}}{\partial z}) - \frac{\partial(\omega \cdot X_{aDom})}{\partial z} \tag{S1g}$$

$$\frac{\partial}{\partial t}X_{aRes} = F^{sorp}_{dom\to aDom} - \frac{\partial}{\partial z}(D_b\frac{\partial X_{aRes}}{\partial z}) - \frac{\partial(\omega \cdot X_{aRes})}{\partial z} \tag{S1h}$$

where $F_{L_{vp}}$ is the litterfall of the various plant tissue types, $f_{vp\to i}$ are the coefficients determining the partitioning of this litterfall to the litter pools (see Section S1.1), τ_i are temperature and moisture adjusted turnover times of the respective pools (X; i = sol, wl, mic), $\eta_{i\to j}$ are the fractions of mass transfer from pool i to j (see Section S1.2), $F^Y_{i\to j}$ is the the flux rates of processes Y ($depoly$: depolymerisation; upt: microbial uptake of DOM; $sorp$: sorption to mineral surface) from pool i to j (see Section S1.4, S1.3 and S1.5), F^{growth}_{mic} the microbial growth rate, $\sigma_{recycle}$ is the additional nutrients recycled to DOM when microbes decay, $\Phi_{immobilisation}$ is the immobilisation terms for N and P, required to balance the microbial C:N:P stoichiometry (see Sect. S1.5). The D_b is a prescribed diffusion constant for transfer of soil organic matter through bioturbation, and ω is the flux rate representing the advective transport of soil organic matter due to SOM accumulation/diminishing, where the above-ground woody litter is not subjective to this transport (see Section S3), and $\frac{\partial v_{dom} dom}{\partial z}$ is the percolation loss term given by the dom concentration and water mass flow between soil layers.

S1.1 Partitioning of litterfall to litter pools

Non-woody litterfall is partitioned to the soluable and polymeric litter according to the CENTURY approach (Parton et al., 1993). Litter from labile and reserve pools is assumed to enter the soluable pools, litter from sap- and heartwood enters the woody pool. The soluable fraction of litterfall from each vegetation pool ($_{vp}$, i.e. leaves, fine and coarse roots, fruits and seed-bed) is determined as:

$$f_{vp\to sol,C} = f_{sol,max,C} - k_{sol,C} \cdot LC_{vp} \frac{C_{vp}}{N_{vp}} \tag{S2}$$

where $f_{vp\to sol,C}$ is constrained to positive solutions, $f_{sol,max,C}$ is the maximum fraction allocated to the soluable pool, $k_{sol,C}$ a factor relating the soluable litter fraction to the lignin to nitrogen ratio, LC_{vp} the tissue-specific fraction of the lignin content of that tissue type, and $\frac{C_{vp}}{N_{vp}}$ the C:N ratio of litterfall from that tissue. The lignin content is assumed constant for all but the leaf tissues. For the latter, an empirical dependency between lignin content and specific leaf-area (sla) is used (White et al., 2000).

$$LC_{leaf} = LC_{leaf,max} + k_{leaf2sla} \cdot sla \tag{S3}$$

The remainder of litterfall is allocated to the polymeric pool. For N and P, the partitioning assumes that the relative proportions of C:N and N:P are preserved in the partitioning according to:

$$f_{vp\to sol,X} = \frac{1}{1 + \frac{1 - f_{vp\to sol,C}}{k_{sol,vp,X} \cdot f_{vp\to sol,C}}} \tag{S4}$$

S1.2 Litter turnover

Woody decomposition is assumed to be a two-stage process. The first step implies physical destabilisation and a first level of biochemical processing, which releases a constant fraction of carbon (1 - $\eta_{C,wl\to poly}$) to heterotrophic respiration. The remainder is assumed to enter the polymeric litter that further depolymerises into DOM. soluable litter decomposes with a similar two-stage process, where during the first step a fraction of carbon (1 - $\eta_{C,sol\to dom}$) is respired but the remainder directly enters the DOM pool, which is taken up by microbes.

The turnover times (τ_i^{base}) of the woody and soluable litter respond to soil temperature (T_{soil}) and soil water content (Θ) as follows:

$$\tau_i^* = \tau_i^{base} f(T_{soil}) g(\Theta_{soil}),\ where \tag{S5a}$$

$$f(T_{soil}) = e^{-\frac{E_{a,depoly}}{R}(\frac{1}{T_{soil}} - \frac{1}{T^r_{ref}})} \tag{S5b}$$

$$g(\Theta) = \frac{afps^{k1_{afps}}}{k_{afps} + afps^{k1_{afps}}},\ where \tag{S5c}$$

$$afps = \frac{\Theta_{fc} - \Theta_{soil}}{\Theta_{fc}} \tag{S5d}$$

where $E_{a,depoly}$ is the activation energy of depolymerisation, T^{τ}_{ref} is the reference temperature of the turnover rate, $k1_{afps}$ and k_{afps} are parameters, $afps$ is the air filled pore space, and Θ_{soil} and Θ_{fc} are the absolute soil water content and soil water field capacity, respectively.

S1.3 Depolymerisation

The depolymerisation from polymeric litter or microbial residue to DOM (dom) are assumed to be enzyme-limited and described with "reverse Michaelis-Menten" kinetics ((Ahrens et al., 2015), (Schimel and Weintraub, 2003)).

$$F^{depoly}_{poly\rightarrow dom} = v^{poly}_{max,depoly}(T_{soil},\Theta)\frac{X_{mic}Enz^{poly}_{frac}}{K_{m,depoly}(T_{soil},\Theta)+X_{mic}Enz^{poly}_{frac}}X_{poly} \tag{S6a}$$

$$F^{depoly}_{res\rightarrow dom} = v^{res}_{max,depoly}(T_{soil},\Theta)\frac{X_{mic}Enz^{res}_{frac}}{K_{m,depoly}(T_{soil},\Theta)+X_{mic}Enz^{res}_{frac}}X_{res},\ where \tag{S6b}$$

$$K_{m,depoly}(T_{soil},\Theta) = K_{m,depoly}e^{-\frac{Ea,hsc}{R}(\frac{1}{T_{soil}}-\frac{1}{T^{\tau}_{ref}})}\cdot(\frac{\Theta}{\Theta_{fc}})^{k_{hsc}} \tag{S6c}$$

where $v^{X}_{max,depoly}$ is the maximum depolymerisation rate of pool X ($poly$ or res) and its temperature and moisture responses are the same as those of litter turnover (Eq.S5), Enz^{X}_{frac} is the fraction of enzyme (see Sect.S1.5.2) which targets to depolymerise pool X, and $K_{m,depoly}(T_{soil},\Theta)$ is the temperature and moisture corrected, microbial biomass scaled, half-saturation enzyme concentration of depolymerisation.

S1.4 SOC sorption stabilisation

The sorption of DOM and microbial residue to mineral soil surface is represented with dynamic Langmuir isotherm, modified from the COMISSION model (Ahrens et al., 2015).

$$F^{sorp}_{dom\rightarrow aDom} = k^{ads}_{dom}X_{dom}f(T_{soil},\Theta)Q^{org}_{avail} + k^{des}_{dom}f(T_{soil},\Theta)X_{aDom} \tag{S7a}$$

$$F^{sorp}_{res\rightarrow aRes} = k^{ads}_{res}X_{res}f(T_{soil},\Theta)Q^{org}_{avail} + k^{ads}_{res}f(T_{soil},\Theta)X_{aRes},\ where \tag{S7b}$$

$$f(T_{soil},\Theta) = e^{-\frac{Ea,sorption}{R}(\frac{1}{T_{soil}}-\frac{1}{T^{\tau}_{ref}})}\cdot\frac{\Theta}{dz} \tag{S7c}$$

$$Q^{org}_{avail} = Q^{org}_{max} - X_{aDom} - X_{aRes} \tag{S7d}$$

$$Q^{org}_{max} = q^{org}_{max,mineral}\cdot(Silt+Clay)\rho_{soil}V^{frac}_{mineral} \tag{S7e}$$

where k^{ads}_{X} and k^{des}_{X} are the adsorption rate and desorption rate between X (dom or res) and its mineral-associated form ($aDom$ or $aRes$), respectively, dz is the soil depth, and $Silt$ and $Clay$ are the silt and clay content in weight fraction. It is assumed that the two substrates share the same sorption sites, which is represented by the maximum sorption capacity of organic matter Q^{org}_{avail} and it is calculated based on the weight and sorption capacity of fine soil, $q^{org}_{max,mineral}$, following COMISSION (Ahrens et al., In prep.).

S1.5 Microbial growth and decay

In JSM, the growth of microbial biomass (F^{growth}_{mic}) depends on three factors: i) the uptake rate of DOM ($F^{upt}_{dom\rightarrow mic}$), ii) the microbial carbon use efficiency (CUE), mic^{mavg}_{cue}, and iii) nutrient (N and P) limitation, $scal_{C,N,P\ limit}$.

$$F^{growth}_{mic} = mic^{mavg}_{cue}F^{upt}_{dom\rightarrow mic} \tag{S8a}$$

$$F^{upt}_{dom\rightarrow mic} = MIN(F^{upt^{*}}_{dom\rightarrow mic}, scal_{C,N,P\ limit}\cdot C_{dom}) \tag{S8b}$$

The potential uptake of DOM, $F^{upt^*}_{dom\rightarrow mic}$, is constrained by the DOM concentration, meaning at high DOM concentration the uptake is limited by ability of microbes to assimilate DOM (Ahrens et al., 2015). It is described with "Michaelis-Menten" kinetics,

$$F^{upt^*}_{dom\rightarrow mic} = v^{dom}_{max,upt}(T_{soil},\Theta)C_{mic}\frac{C_{dom}}{K_{m,upt}(T_{soil},\Theta)+C_{dom}} \tag{S9a}$$

$$K_{m,upt}(T_{soil},\Theta) = K_{m,upt}e^{-\frac{Ea,hsc}{R}(\frac{1}{T_{soil}}-\frac{1}{T^*_{ref}})}\cdot(\frac{\Theta}{\Theta_{fc}})^{k_{hsc}} \tag{S9b}$$

where $v^{dom}_{max,upt}$ is the maximum DOM uptake rate and has the same temperature and mositure responses as those of litter turnover (Eq.S5), $K_{m,upt}(T_{soil},\Theta)$ is the temperature and moisture corrected half-saturation coefficient for DOM uptake.

Microbes response to the instantaneous conditions and associated fluxes to adapt their CUE. It is assumed in JSM that all the microbial adaptation has a process-specific lag time. Therefore, the microbial growth is calculated using the time-averaging microbial CUE, mic^{mavg}_{cue}, which is a moving average of the current effective microbial CUE (mic^{eff}_{cue}) over a certain lag time.

$$mic^{mavg,new}_{cue} = mic^{mavg,old}_{cue}\cdot(1-\frac{dt}{\tau^{mic}_{mavg}})+mic^{eff}_{cue}\cdot\frac{dt}{\tau^{mic}_{mavg}} \tag{S10a}$$

$$mic^{eff}_{cue} = MAX(mic^{min}_{cue},\frac{F^{growth^*}_{mic}}{F^{upt^*}_{dom\rightarrow mic}}) \tag{S10b}$$

$$F^{growth^*}_{mic} = MIN(F^{growth,C^*}_{mic},F^{growth,N^*}_{mic},F^{growth,P^*}_{mic}),\ where \tag{S10c}$$

$$F^{growth,C^*}_{mic} = mic^{max}_{cue}F^{upt^*}_{dom\rightarrow mic} \tag{S10d}$$

$$F^{growth,N^*}_{mic} = (mic_{nue}\frac{F^{upt^*}_{dom\rightarrow mic}}{\chi^{C:N}_{dom}}+U^*_{NO_3,mic}+U^*_{NH_4,mic})\chi^{C:N}_{mic} \tag{S10e}$$

$$F^{growth,P^*}_{mic} = (mic_{pue}\frac{F^{upt^*}_{dom\rightarrow mic}}{\chi^{C:P}_{dom}}+U^*_{PO_4,mic})\chi^{C:P}_{mic} \tag{S10f}$$

where τ^{mic}_{mavg} is the time span of the microbial CUE acclimation, mic^{min}_{cue} is the theoretical minimal microbial CUE, F^{growth,X^*}_{mic} is the maximum potential microbial growth rate only considering the availability of element X, which takes account of the microbial nitrogen and phosphorus use efficiencies, mic_{nue} and mic_{pue} [1], and the potential microbial uptake rate of nutrient, $U^*_{X,mic}$ (X=NO_3, NH_4, PO_4, see Sect.S2.2). The smallest growth potential determines the current effective CUE.

Given the time-averaging microbial CUE, the potential microbial growth only considering C is recalculated as $F^{growth,C^{**}}_{mic}$. The uptake rate of DOM will be reduced if $F^{growth,C^{**}}_{mic}$ is bigger than F^{growth,X^*}_{mic}, and the scaling factor $scal_{C,N,P\ limit}$ is calculated as,

$$scal_{C,N,P\ limit} = \begin{cases} MIN\left(\frac{F^{upt^*}_{dom\rightarrow mic}}{C_{dom}},\ \frac{(U^*_{NO_3,mic}+U^*_{NH_4,mic})\chi^{C:N}_{mic}}{mic^{mavg}_{cue}C_{dom}-mic_{nue}N_{dom}\chi^{C:N}_{mic}}\right),\ if\ F^{growth,N^*}_{mic} < F^{growth,C^{**}}_{mic}\&F^{growth,P^*}_{mic} \\ MIN\left(\frac{F^{upt^*}_{dom\rightarrow mic}}{C_{dom}},\ \frac{U^*_{PO_4,mic}\chi^{C:P}_{mic}}{mic^{mavg}_{cue}C_{dom}-mic_{pue}P_{dom}\chi^{C:P}_{mic}}\right),\ if\ F^{growth,P^*}_{mic} < F^{growth,C^{**}}_{mic}\&F^{growth,N^*}_{mic} \end{cases} \tag{S11a}$$

$$where,\ F^{growth,C^{**}}_{mic} = mic^{mavg}_{cue}F^{upt^*}_{dom\rightarrow mic} \tag{S11b}$$

[1] In Eq.S10f and all the following cases, the microbial $\chi^{C:P}_{mic} = \chi^{C:N}_{mic}\cdot\chi^{N:P}_{mic}$

S1.5.1 Microbial nutrient uptake, mineralisation, and microbial recycle

Given the microbial growth and the C:N:P stoichiometry, the uptake of inorganic N and P, $U_{X,mic}$, is calculated as,

$$U_{NH_4,mic} = U^*_{NH_4,mic} scal_N \tag{S12a}$$

$$U_{NO_3,mic} = U^*_{NO_3,mic} scal_N \tag{S12b}$$

$$U_{PO_4,mic} = U^*_{PO_4,mic} scal_P, \ where \tag{S12c}$$

$$scal_N = \frac{MAX(\frac{F^{growth,C}_{mic}}{\chi^{C:N}_{mic}} - mic_{nue} F^{upt,N}_{mic}, \ 0.0)}{U^*_{NO_3,mic} + U^*_{NH_4,mic}},$$

$$\text{If } F^{growth,C}_{mic} \leq F^{growth,N^{**}}_{mic} \tag{S12d}$$

$$scal_P = \frac{MAX(\frac{F^{growth,C}_{mic}}{\chi^{C:P}_{mic}} - mic_{pue} F^{upt,P}_{mic}, \ 0.0)}{U^*_{PO_4,mic}}$$

$$\text{If } F^{growth,C}_{mic} \leq F^{growth,P^{**}}_{mic} \tag{S12e}$$

$$F^{upt,N}_{mic} = mic^{mavg}_{cue} \frac{F^{upt}_{dom \to mic}}{\chi^{C:N}_{dom}} \tag{S12f}$$

$$F^{upt,P}_{mic} = mic^{mavg}_{cue} \frac{F^{upt}_{dom \to mic}}{\chi^{C:P}_{dom}} \tag{S12g}$$

$$F^{growth,N^{**}}_{mic} = (F^{upt,N}_{mic} + U^*_{NO_3,mic} + U^*_{NH_4,mic}) \chi^{C:N}_{mic} \tag{S12h}$$

$$F^{growth,P^{**}}_{mic} = (F^{upt,P}_{mic} + U^*_{PO_4,mic}) \chi^{C:P}_{mic} \tag{S12i}$$

where $F^{growth,N^{**}}_{mic}$ and $F^{growth,P^{**}}_{mic}$ are the potential microbial growth only considering N or P availability given the time-averaging CUE.

The effective microbial nutrient use efficiency (mic^{eff}_{nue} and mic^{eff}_{pue}) and the net mineralisation of N and P (Φ^{net}_{NorP}) are thus calculated as,

$$mic^{eff}_{nue} = MIN(mic_{nue}, \frac{\frac{F^{growth,C}_{mic}}{\chi^{C:N}_{mic}} - U_{NH_4,mic} - U_{NO_3,mic}}{F^{upt,N}_{mic}}) \tag{S13a}$$

$$mic^{eff}_{pue} = MIN(mic_{pue}, \frac{\frac{F^{growth,C}_{mic}}{\chi^{C:P}_{mic}} - U_{PO_4,mic}}{F^{upt,P}_{mic}}) \tag{S13b}$$

$$\Phi^{net}_{NH_4} = (1 - mic^{eff}_{nue}) F^{upt,N}_{mic} - U_{NH_4,mic} \tag{S13c}$$

$$\Phi^{net}_{NO_3} = -U_{NO_3,mic} \tag{S13d}$$

$$\Phi^{net}_{PO_4} = (1 - mic^{eff}_{pue}) F^{upt,P}_{mic} - U_{PO_4,mic} \tag{S13e}$$

When microbes decay in JSM, there is a faction of the dead microbes ($\eta_{mic \to dom}$) which directly recycles into the DOM pool and the rest ($\eta_{mic \to res}$) become microbial residues. Due to the fact that microbial cell wall has a lower nutrient content than plasma, it is assumed in JSM that N and P are more prone to be recycled into DOM when microbes decay, which is represented by $\sigma_{recycle}$ in Eq.S1.

$$\sigma^X_{recycle} = \eta_{mic \to res} \frac{X_{mic}}{\tau_{mic}} \eta^X_{res \to dom} \tag{S14a}$$

where X represents N or P, and $\eta^X_{res\rightarrow dom}$ is the fraction of X that is recycled from newly formed res to dom during microbial decay.

S1.5.2 Enzyme allocation in depolymerisation

The enzyme allocation to polymeric litter and microbial residue is presented with the steady state of the Revenue strategy in the SEAM model (Wutzler et al., 2017), assuming that the microbial community adapts in a way that the fraction of enzyme allocation is proportional to its revenue (return-investment rate) of the limiting elements (C, N, or P).

$$\alpha^X_{poly} = \frac{Rev^X_{poly}}{Rev^X_{poly} + Rev^X_{res}} \tag{S15a}$$

$$\alpha^X_{res} = \frac{Rev^X_{res}}{Rev^X_{poly} + Rev^X_{res}},\ where \tag{S15b}$$

$$Rev^X_{poly} = \frac{return}{investment} = \frac{v^{poly}_{max,depoly} \cdot \frac{\alpha^X_{poly} C_{mic}}{K_{m,depoly} + \alpha^X_{poly} C_{mic}} \cdot X_{poly}}{\alpha^X_{poly} C_{mic}}$$

$$= \frac{v^{poly}_{max,depoly}}{K_{m,depoly} + \alpha^X_{poly} C_{mic}} X_{poly} \tag{S15c}$$

$$Rev^X_{res} = \frac{v^{res}_{max,depoly}}{K_{m,depoly} + \alpha^X_{res} C_{mic}} X_{res},\ and \tag{S15d}$$

$$\alpha^X_{poly} + \alpha^X_{res} = 1 \tag{S15e}$$

where α^X_Y is the potential enzyme allocation fraction to Y ($poly$ or res) based on the revenues of element X (C, N, or P), and Rev^X_y is the revenue of element X from source y and is defined as the production of X divided by the potential allocation of enzyme. In JSM the enzyme levels are not explicitly represented, thus a steady state assumption is made: the production and turnover of the enzyme is in equilibrium therefore the enzyme is always linear with the microbial biomass. we could get the analytical solution of the potential enzyme allocation fractions by rearranging Eq.S15,

$$\frac{\alpha^X_{poly}}{\alpha^X_{res}} = \frac{Rev^X_{poly}}{Rev^X_{res}} \Longrightarrow \tag{S16a}$$

$$\frac{v^{poly}_{max,depoly} X_{poly}}{v^{res}_{max,depoly} X_{res}} = \frac{\alpha^X_{poly}}{1 - \alpha^X_{poly}} \frac{K_{m,depoly} + \alpha^X_{poly} C_{mic}}{K_{m,depoly} + (1 - \alpha^X_{poly}) C_{mic}} \Longrightarrow \tag{S16b}$$

$$\alpha^X_{poly} = \frac{d_{poly} K_{m,depoly} + 2 d_{poly} C_{mic} + d_{res} K_{m,depoly} - \sqrt{D}}{2 C_{mic} (d_{poly} - d_{res})}, where \tag{S16c}$$

$$d_{poly} = v^{poly}_{max,depoly} X_{poly} \tag{S16d}$$

$$d_{res} = v^{res}_{max,depoly} X_{res} \tag{S16e}$$

$$D = 4 d_{poly} d_{res} C^2_{mic} + 8 d_{poly} d_{res} C_{mic} K_{m,depoly} + K^2_{m,depoly} d^2_{poly} + 2 d_{poly} d_{res} K^2_{m,depoly} + K^2_{m,depoly} d^2_{res} \tag{S16f}$$

It is assumed that the microbial community would acclimate gradually to allocate the enzyme to optimize the utilisation of the most limiting element of depolymerisation, which is determined similarly as that in microbial growth (Eq.S10) except that the uptake of inorganic nutrients are not considered.

$$Enz_{frac}^{poly,new} = Enz_{frac}^{poly,old} \cdot (1 - \frac{dt}{\tau_{mavg}^{enzyme}}) + \alpha_{poly,mavg}^{X,new} \cdot \frac{dt}{\tau_{mavg}^{enzyme}},\ where \tag{S17a}$$

$$\alpha_{poly,mavg}^{X,new} = \alpha_{poly,mavg}^{X,old} \cdot (1 - \frac{dt}{\tau_{mavg}^{enzyme}}) + \alpha_{poly}^{X} \cdot \frac{dt}{\tau_{mavg}^{enzyme}} \tag{S17b}$$

and the most limiting element X is determined as (S17c)

$$\begin{aligned} MIN\Big(& (F_{poly\to dom}^{depoly} + F_{res\to dom}^{depoly}) \cdot mic_{cue}^{mavg}, \\ & (\frac{F_{poly\to dom}^{depoly}}{\chi_{poly}^{C:N}} + \frac{F_{res\to dom}^{depoly}}{\chi_{res}^{C:N}}) \cdot mic_{nue}^{mavg} \chi_{mic}^{C:N}, \\ & (\frac{F_{poly\to dom}^{depoly}}{\chi_{poly}^{C:P}} + \frac{F_{res\to dom}^{depoly}}{\chi_{res}^{C:P}}) \cdot mic_{pue}^{mavg} \chi_{mic}^{C:P} \Big) \end{aligned} \tag{S17d}$$

where τ_{mavg}^{enzyme} is the time span of enzyme allocation acclimation, and mic_{nue}^{mavg} and mic_{pue}^{mavg} are the time averaging microbial N and P use efficiency, which is calculated similarly as mic_{cue}^{mavg} in Eq.S10.

S2 Inorganic nutrient cycles

In JSM, the net mineralisation and plant uptake of NH_4 and NO_3 are represented next to transport process. The dynamics of inorganic nitrogen are described as:

$$\begin{aligned} \frac{\partial}{\partial t} NH_4 = & F_{dep,NH_4} - U_{NH_4,plant} + \Phi_{NH_4}^{net} \\ & - \frac{\partial}{\partial z}(D_b \frac{\partial NH_4}{\partial z}) - \frac{\partial(\omega \cdot NH_4)}{\partial z} - \frac{\partial v_{NH_4} NH_4}{\partial z} \end{aligned} \tag{S18a}$$

$$\begin{aligned} \frac{\partial}{\partial t} NO_3 = & F_{dep,NO_3} - U_{NO_3,plant} + \Phi_{NO_3}^{net} \\ & - \frac{\partial}{\partial z}(D_b \frac{\partial NO_3}{\partial z}) - \frac{\partial(\omega \cdot NO_3)}{\partial z} - \frac{\partial v_{NO_3} NO_3}{\partial z} \end{aligned} \tag{S18b}$$

where U are the uptake rates of plants and microbes (see Section S2.2); the $F_{dep,X}$ are the atmospheric deposition fluxes; $\frac{\partial v_x X}{\partial z}$, $\frac{\partial}{\partial z}(D_b \frac{\partial X}{\partial z})$, and $\frac{\partial(\omega \cdot X)}{\partial z}$ are vertical transport terms due to percolation loss, bioturbation, and SOM accumulation/diminishing, respectively (see Sect.S3).

The inorganic phosphorus cycle is mostly based on that of the QUINCY model (Thum et al., 2019) with modifications due to microbial interactions. The dynamics of inorganic phosphorus are described as:

$$\begin{aligned}\frac{\partial}{\partial t}PO_4 &= F_{dep,PO_4} + F_{weath,PO_4} + F_{biomin,PO_4} \\ &\quad - U_{plant,PO_4} - F_{adsorp,PO_4} + \Phi^{net}_{PO_4} \\ &\quad - \frac{\partial}{\partial z}(D_b \frac{\partial PO_4}{\partial z}) - \frac{\partial(\omega \cdot PO_4)}{\partial z} - \frac{\partial v_{PO_4} PO_4}{\partial z} \end{aligned} \tag{S19a}$$

$$\frac{\partial}{\partial t}P_{lab} = F_{adsorp,PO_4} - F_{absorb,PO_4} - \frac{\partial(\omega \cdot P_{lab})}{\partial z} \tag{S19b}$$

$$\frac{\partial}{\partial t}P_{sorb} = F_{absorb,PO_4} - F_{occlusion,PO_4} - \frac{\partial(\omega \cdot P_{sorb})}{\partial z} \tag{S19c}$$

$$\frac{\partial}{\partial t}P_{ocl} = F_{occlusion,PO_4} - \frac{\partial(\omega \cdot P_{ocl})}{\partial z} \tag{S19d}$$

$$\frac{\partial}{\partial t}P_{primary} = -F_{weath,PO_4} - \frac{\partial(\omega \cdot P_{primary})}{\partial z} \tag{S19e}$$

where P_{lab}, P_{sorb}, P_{ocl}, and $P_{primary}$ are adsorbed, absorbed, occluded, and primary P, respectively; the F_{dep,PO_4}, F_{weath,PO_4}, F_{biomin,PO_4}, F_{adsorp,PO_4}, and F_{absorb,PO_4} are the atmospheric deposition, weathering, fast adsorption, and absorption fluxes, respectively (see Section S2.1).

S2.1 Phosphorus weathering, biomineralisation and absorption

Weathering is assumed to be driven by root and microbial exudation, and modified from Wang et al. (2010) as:

$$F_{weath,PO_4} = f(T_{soil}, \Theta) \frac{C_{exu}}{K_{m,weath} + C_{enz}} k_{weath} \rho^{cor}_{soil}, \; where \tag{S20a}$$

$$f(T_{soil}, \Theta) = e^{-\frac{Ea,hsc}{R} \cdot (\frac{1}{T_{soil}} - \frac{1}{T^{*}_{ref}})} \cdot (\frac{\Theta}{\Theta_{fc}})^3, \tag{S20b}$$

$$C_{exu} = C_{fine\_root} k_{enz,root} + C_{mic} k_{enz,mic} \tag{S20c}$$

where k_{weath} is the rate constant for weathering, ρ^{cor}_{soil} is the soil bulk density corrected by SOM content, C_{exu} represents an implicit general assemble of all exudation, analogous to the enzymatic abundance of fine roots and microbes ($k_{enz,root}$ and $k_{enz,mic}$), and $K_{m,weath}$ is the half-saturation coefficient for weathering. The weathering rate decreases with soil depth as the fine root C and microbial biomass decreases and is modified by soil temperature and moisture.

The biomineralisation of PO_4 is determined as an additional enzyme-catalysed cleavage of the P contained in the solid SOM pools (X = res, $aRes$, $aDom$), modified by temperature and moisture modifiers, affected by the concentration of PO_4 and enzyme abundance, and constrained by the C:P ratio of the organic pools:

$$F_{biomin,PO_4} = v_{max,biomin} f(T_{soil}, \Theta) f(C_{enz} f(PO_4) f(\chi^{C:P}_X), \; where \tag{S21a}$$

$$f(C_{enz}) = \frac{C_{enz}}{K^{exu}_{m,biomin} + C_{enz}} \tag{S21b}$$

$$f(PO_4) = \frac{K^{PO_4}_{m,biomin}}{K^{PO_4}_{m,biomin} + PO_4} \tag{S21c}$$

$$f(\chi^{C:P}_X) = \frac{1}{1 + \chi^{C:P}_X K^{CP}_{m,biomin}} \tag{S21d}$$

where $K_{m,biomin}$, $K^{PO_4}_{m,biomin}$ and $K_{m,P:C}$ are constants constraining the biomineralisation rate under low enzyme, high PO_4 concentration, and high SOM C:P ratio, respectively, $\chi^{C:P}_X$ is the C:P ratio of the organic pools, and the temperature and moisture responses are calculated as those in Eq. S5.

PO_4 absorption and occlusion are modelled as:

$$F_{occlusion,PO_4} = k_{ocl} P_{sorb} \tag{S22a}$$

$$F_{desorp,PO_4} = f(T_{soil}, E_{a,abs}) k_{abs} P_{lab} - f(T_{soil}, E_{a,des}) k_{s,des} P_{sorb},\ where \tag{S22b}$$

$$f(T_{soil,E_a}) = e^{-\frac{E_a}{R} \cdot (\frac{1}{T_{soil}} - \frac{1}{T^*_{ref}})} \tag{S22c}$$

where k_{ocl}, k_{abs} and $k_{s,des}$ are the rate constants of occlusion, absorption and slow desorption, and $E_{a,abs}$ and $E_{a,des}$ are the respective activation energies which equal to that of OM sorption (Eq.S7).

S2.2 Nutrient acquisition

It is assumed in the JSM model that the soluble forms of inorganic NH_4, NO_3, and PO_4 are the only bio-available nutrients for plants and microbes, and specifically for PO_4, the soluble inorganic form is assumed to be the only form that could be adsorbed by the mineral surfaces. The uptake of plants and microbes as well as the PO_4 adsorption are all represented by the formations of consumer-substrate network using their full equilibrium chemistry approximations (ECA), following Tang and Riley (2013):

$$U^*_{X,y_1} = f(T_{soil}, \Theta)_{y_1} v^X_{max,y_1} \frac{[X]}{K^X_{m,y_1} + [X] + Enz^X_{y_1} + K^X_{m,y_1} \frac{Enz^X_{y_2}}{K^X_{m,y_2}} + K^X_{m,y_1} \frac{Enz^X_{y_3}}{K^X_{m,y_3}}},\ where \tag{S23a}$$

$$Enz^X_{plant} = C_{fine\_root} k^X_{enz,root} \tag{S23b}$$

$$Enz^X_{mic} = C_{mic} k^X_{enz,mic} \tag{S23c}$$

Specificlly, for PO_4 adsorption flux we assumed (S23d)

$$Enz^{PO_4}_{adsorp} = S^{PO_4}_{max} - P_{lab} \tag{S23e}$$

$$v^{PO_4}_{max,adsorp} = k_{ads} \cdot Enz^{PO_4}_{adsorp} \cdot PO_4 \tag{S23f}$$

$$k_{ads} = \frac{k_{des,f}}{K_S} \tag{S23g}$$

$$[PO_4] = P_{lab} + PO_4 \tag{S23h}$$

where $U^*_{X,y}$ is the potential acquisition rate of substrate X (NH_4, NO_3, and PO_4) through process y ($plant$: plant uptake, mic: microbial uptake, or $adsorp$: adsorption). The maximum uptake rates ($v^X_{max,y}$) of plant and microbes are adopted from literature (see Table S1), while the maximum PO_4 adsorption rate is calculated following Van der Zee et al. (1989); Enz^X_y represents the enzymatic capacity of y to consume the substrate X and it is assumed to be linear with the root biomass of plant, microbial biomass for microbe, and equals with the available sorption sites for mineral soil, and $k^X_{enz,y}$ is the coefficient representing the transporters' abundance and capacity; the $[X]$ represents the total substrate concentration for all the relevant acquisition processes, and it equals the soluble inorganic concentration for NH_4 and NO_3, while for PO_4 it is the sum of soluble and labile inorganic P. The uptake rate of plants and microbes are influenced by temperature and moisture as that in Eq.S6.

The potential acquisition rate will be down scaled if the sum of them exceed the size of the substrate pool. The actual microbial uptake rate also depends on the uptake demand of microbes (see Sect.S1.5). The actual adsorption rate are further calculated based on the assumption that the soluble inorganic P tend to equilibrate with the adsorbed P (see Sect.S2.2.1).

$$U^*_{X,y_1} = U^*_{X,y_1} \cdot \frac{X}{\sum(U^*_{X,y})} \; when \; X < \sum(U^*_{X,y}) \tag{S24a}$$

S2.2.1 PO_4 adsorption equilibrium

The adsorption (F_{adsorp,PO_4}) flux from soil solution to the soil adsorption sites is calculated assuming constant Langmuir equilibrium (Barrow, 1978) between soluble and adsorbed P:

$$PO_4 = \frac{S^{PO_4}_{max} \cdot PO_4}{K_S + PO_4}, \; where \tag{S25a}$$

$$S^{PO_4}_{max} = \Theta_{soil} \cdot (S^{PO_4}_{max,om} V^{frac}_{om} \rho^{org}_{bulk} + S^{PO_4}_{max,mineral} V^{frac}_{mineral} \rho_{soil}) \tag{S25b}$$

$$K_S = K_{S,om} V^{frac}_{om} \rho^{org}_{bulk} + K_{S,mineral} V^{frac}_{mineral} \rho_{soil} \tag{S25c}$$

where $S^{PO_4}_{max}$ and K_S are the maximum sorption capacity, and the half-saturation concentration coefficient of the soil, and are both modified by soil moisture and SOM content; V^{frac}_{om} and $V^{frac}_{mineral}$ are volumetric fractiosn of organic matter and fine soil minerals, respectively. $S^{PO_4}_{max,om}$ and $S^{PO_4}_{max,mineral}$ are the maximum PO_4 sorption capacity of pure organic matter and pure fine soil, respectively. $K_{S,om}$ and $K_{S,mineral}$ are the half-saturation concentration coefficient of pure organic matter and pure fine soil, respectively.

The Eq.S25 is solved analytically since $S^{PO_4}_{max}$ and K_S are also changing with time.

$$P^{'}_{lab} = \frac{[PO_4]^{'} + S^{PO_4}_{max} + K_S - \sqrt{([PO_4]^{'} + S^{PO_4}_{max} + K_S)^2 - 4 \cdot [PO_4]^{'} S^{PO_4}_{max}}}{2} \tag{S26a}$$

$$PO^{'}_4 = [PO_4]^{'} - P_{lab}, \; where \tag{S26b}$$

$$[PO_4]^{'} = P_{lab} + PO_4 + \frac{\partial(P_{lab} + PO_4)}{\partial t} \tag{S26c}$$

$$\begin{aligned} \frac{\partial(P_{lab} + PO_4)}{\partial t} &= F_{dep,PO_4} + F_{weath,PO_4} + F_{biomin,PO_4} \\ &- U_{plant,PO_4} - U_{mic,PO_4} + \Phi^{net}_{PO_4} \\ &- \frac{\partial}{\partial z}(D_b \frac{\partial PO_4}{\partial z}) - \frac{\partial(\omega \cdot PO_4)}{\partial z} - \frac{\partial v_{PO_4} PO_4}{\partial z} \\ &- F_{absorb,PO_4} - \frac{\partial(\omega \cdot P_{lab})}{\partial z} \end{aligned} \tag{S26d}$$

where the pools with apostrophe as superscript denote the size at the end of time step.

S3 Transport and bulk density correction

In JSM the soil profile always starts from the top of the organic layer, therefore changes of SOM content would affect the layering of the soil profile, which is represented by an advective transport rate ω, following COMISSION model Ahrens et al. (2015)

$$\omega_{sl=n} = \frac{\sum_{sl=n}^{1} \Delta W_{OM_{sl}} \cdot dz_{sl}}{\rho_{bulk}^{org}},\ where \tag{S27a}$$

$$\Delta W_{OM_{sl}} = \sum \left(C'_{X_{sl}} - C_{X_{sl}}\right) \frac{Mol_C}{1000 \cdot frac_{OM}^{C}} \tag{S27b}$$

where subscript sl denotes the soil layer, dz the layer depth, ρ_{bulk}^{org} the bulk density of organic material; ΔW_{OM} is the change of total SOM weight which includes all the organic pools (NOTE: for the first layer woody litter is excluded), and is calculated based on the change of C content ($C'_{X_{sl}} - C_{X_{sl}}$), carbon molecular weight (Mol_C) and weight fraction of C in OM ($frac_{OM}^{C}$).

Not only all the organic pools and inorganic pools shift with the advective transport rate ω in JSM, but also the physical soil properties, such as soil texture, mineral soil density (ρ_{soil}) and mineral soil volumetric fraction ($V_{mineral}^{frac}$), shift with ω to ensure that the soil bulk density is properly corrected by the SOM content.

$$\rho_{soil}^{cor} = V_{mineral}^{frac} \rho_{soil} + (1 - V_{mineral}^{frac}) \rho_{bulk}^{org} \tag{S28a}$$

Table S1. JSM parameters

Symbol	Description	Value	Unit	Equation	Citation
Litter partitioning and turnover					
$f_{sol,max,C}$	maximum fraction of soluble litter formation	0.85	-	S2	Parton et al. (1993)
$k_{sol,C}$	slope of soluble fraction with lignin to N ratio	0.018	-	S2	Parton et al. (1993)
LC_{fine_root}	lignin content of fine root	0.2565592	mol^{-1}	S2	White et al. (2000)
LC_{coarse_root}	lignin content of coarse roots	0.8163248	mol^{-1}	S2	Thum et al. (2019)
LC_{woody_litter}	lignin content of woody litter	0.8163248	mol^{-1}	S2	White et al. (2000)
LC_{fruit}	lignin content of seed bed	0.2565592	mol^{-1}	S2	Thum et al. (2019)
LC_{seed_bed}	lignin content of fine root	0.2565592	mol^{-1}	S2	Thum et al. (2019)
$LC_{leaf,max}$	maximum lignin content of leaves	0.3440226	mol^{-1}	S3	White et al. (2000)
$k_{leaf2sla}$	slope of lignin to sla relationship	-0.4328854	m^{-2}	S3	Parton et al. (1993)
$k_{sol,vp,N}$	proportionality factor controlling C:N of soluble vs. polymeric pool	5.0	-	S4	Parton et al. (1993)
$k_{sol,vp,P}$	proportionality factor controlling C:P of soluble vs. polymeric pool	5.0	-	S4	Parton et al. (1993)
$\eta_{C,wl\rightarrow poly}$	fraction of woody litter C transformed into polymeric litter	0.3	-	Sect.S1.2	This study
$\eta_{C,sol\rightarrow dom}$	fraction of soluble litter C transformed into DOM	0.7	-	Sect.S1.2	This study
τ_{sol}^{base}	turnover time of soluble litter	0.033	years	S5	Parton et al. (1993)
τ_{wl}^{base}	turnover time of woody litter	2.5	years	S5	Thum et al. (2019)
T_{ref}^{τ}	reference temperature for depolymerisation	293.15	K	S5	Wang et al. (2012)
$E_{a,depoly}$	activation energy for depolymerisation	53000.0	$Jmol^{-1}$	S5	Ahrens et al. (In prep.)
$k1_{afps}$	parameter for moisture response of litter turnover	1.33	-	S5	This study
k_{afps}	parameter for moisture response of litter turnover	0.001	-	S5	This study

Table S1. JSM parameters (ctnd.)

Symbol	Description	Value	Unit	Equation	Citation
Depolymerisation, sorption, transport, and bulk density correction					
$v_{max,depoly}^{poly}$	maximum depolymerisation rate of polymeric litter	0.1849	yr^{-1}	S6	This study
$v_{max,depoly}^{res}$	maximum depolymerisation rate of microbial residue	0.2317	yr^{-1}	S6	This study
$K_{m,depoly}$	half-saturation microbial biomass for depolymerisation	3.70	$\frac{mol}{m^3}$	S6	This study
$E_{a,hsc}$	activation energy of half-saturation point	30000.0	$\frac{J}{mol}$	S6	Wang et al. (2013)
k_{hsc}	scaling factor for the sensitivity of half-saturation constant to moisture limitation	0.001	-	S6	Davidson et al. (2012)
k_{dom}^{ads}	adsorption rate of DOM	0.720	$\frac{m^3}{mol\ yr}$	S7	This study
k_{dom}^{des}	desorption rate of mineral-associated DOM	0.508	yr^{-1}	S7	This study
k_{res}^{ads}	adsorption rate of microbial residue	0.00372	$\frac{m^3}{mol\ yr}$	S7	This study
k_{res}^{des}	desorption rate of mineral-associated residue	0.154	yr^{-1}	S7	This study
$E_{a,sorption}$	activation energy for sorption	5000.0	$Jmol^{-1}$	S7	Ahrens et al. (In prep.)
ρ_{soil}	bulk density of mineral soil	1000 - 1600	$\frac{kg}{m^3}$	S7	Lang et al. (2017)
ρ_{bulk}^{org}	bulk density of organic material	248.84	$\frac{kg}{m^3}$	S28	Lang et al. (2017)
D_b	diffusion velocity due to bioturbation	0.15	$\frac{m^2\ kg}{m^3\ yr}$	S1	Koven et al. (2013)
Microbial growth and decay					
$v_{max,upt}^{dom}$	maximum microbial uptake rate of DOM	95.76	day^{-1}	S8	This study
$K_{m,upt}$	half-saturation DOM density for microbial DOM uptake	85.34	$\frac{mol\ C}{m^3}$	S9	This study
mic_{cue}^{min}	minimal microbial CUE	0.3	-	S10	Manzoni et al. (2008)
mic_{cue}^{max}	maximum microbial CUE	0.6	-	S10	Manzoni et al. (2008)
mic_{nue}	microbial nitrogen use efficiency	0.8	-	S10	Sinsabaugh et al. (2016)
mic_{pue}	microbial phosphorus use efficiency	0.89	-	S10	Sinsabaugh et al. (2016)
$\chi_{mic}^{C:N}$	microbial CN ratio	13	$\frac{mol}{mol}$	S10	Lang et al. (2017)
$\chi_{mic}^{N:P}$	microbial NP ratio	0.8	$\frac{mol}{mol}$	S10	Lang et al. (2017)
τ_{mic}	microbial turnover time	154.7	days	S14	Ahrens et al. (2015)
$\eta_{mic \to res}$	fraction of microbial biomass that become residue during decay	0.828	-	S14	Ahrens et al. (2015)
$\eta_{res \to dom}^{N}$	fraction of N recycled from res to dom during microbial decay	0.4	-	S14	This study
$\eta_{res \to dom}^{P}$	fraction of P recycled from res to dom during microbial decay	0.8	-	S14	This study
τ_{mavg}^{mic}	memory time scale for microbial CUE	30	days	S10	This study
τ_{mavg}^{enzyme}	memory time scale for microbial enzyme allocation	7	days	S17	This study

Table S1. JSM parameters (ctnd.)

Symbol	Description	Value	Unit	Equation	Citation
Nutrient acquisition					
$v_{max,mic}^{nh_4}$	maximum microbial uptake rate of NH_4	1278.7	$\frac{\mu mol\ N}{mol\ C\ h}$	S23	Kuzyakov and Xu (2013)
$v_{max,mic}^{no_3}$	maximum microbial uptake rate of NO_3	1039.0	$\frac{\mu mol\ N}{mol\ C\ h}$	S23	Kuzyakov and Xu (2013)
$K_{m,mic}^{nh_4}$	Half-saturation concentration for microbial NH_4 uptake	0.0129	$\frac{mol\ N}{m^3}$	S23	Kuzyakov and Xu (2013)
$K_{m,mic}^{no_3}$	half+saturation concentration for microbial NO_3 uptake	0.0293	$\frac{mol\ N}{m^3}$	S23	Kuzyakov and Xu (2013)
$k_{enz,mic}^{N}$	coefficient of microbial transporter for N uptake	0.00005	$\frac{mol\ N}{mol\ C}$	S23	Zhu et al. (2016)
$v_{max,plant}^{nh_4}$	maximum plant uptake rate of NH_4	1305.4	$\frac{\mu mol\ N}{mol\ C\ h}$	S23	Kuzyakov and Xu (2013)
$v_{max,plant}^{no_3}$	maximum plant uptake rate of NO_3	218.4	$\frac{\mu mol\ N}{mol\ C\ h}$	S23	Kuzyakov and Xu (2013)
$K_{m,plant}^{nh_4}$	Half-saturation concentration for microbial NH_4 uptake	0.0857	$\frac{mol\ N}{m^3}$	S23	Kuzyakov and Xu (2013)
$K_{m,plant}^{no_3}$	half+saturation concentration for microbial NO_3 uptake	0.129	$\frac{mol\ N}{m^3}$	S23	Kuzyakov and Xu (2013)
$k_{enz,root}^{N}$	coefficient of root transporter for N uptake	0.000125	$\frac{mol\ N}{mol\ C}$	S23	Zhu et al. (2016)
$v_{max,mic}^{po_4}$	maximum microbial uptake rate of PO_4	188.6	$\frac{\mu mol\ P}{mol\ C\ h}$	S23	Zhu et al. (2016)
$K_{m,mic}^{po_4}$	Half-saturation concentration for microbial PO_4 uptake	0.000645	$\frac{mol\ P}{m^3}$	S23	Zhu et al. (2016)
$v_{max,plant}^{po_4}$	maximum microbial uptake rate of PO_4	15.84	$\frac{\mu mol\ P}{mol\ C\ h}$	S23	Kavka and Polle (2016)
$K_{m,plant}^{po_4}$	half-saturation concentration for root PO_4 uptake	0.00216	$\frac{mol\ P}{m^3}$	S23	Kavka and Polle (2016)
$k_{enz,mic}^{P}$	coefficient of microbial transporter for P uptake	0.0005	$\frac{mol\ P}{mol\ C}$	S23	This study
$k_{enz,plant}^{P}$	coefficient of root transporter to take up P	0.000125	$\frac{mol\ P}{mol\ C}$	S23	This study
Soil Pi fluxes					
k_{weath}	Weathering rate constant of mineral soil	8.16208	$10^{-14}\ \frac{molP}{m^3\ s}$	S20	Wang et al. (2010)
$K_{m,weath}$	half-saturation C exudation level for PO_4 weathering	0.083	$\frac{molC}{m^3}$	S20	This study
$v_{max,biomin}$	maximum biomineralisation rate of PO_4	0.005	$\frac{mol\ P}{mol\ C} d^{-1}$	S21	Bünemann et al. (2016)
$K_{m,biomin}^{exu}$	half-saturation C exudation level for PO_4 biomineralization	0.417	$\frac{mol\ C}{m^3}$	S21	This study
$K_{m,biomin}^{PO_4}$	half-saturation solute P concentration for PO_4 biomineralization	0.001	$\frac{mol\ P}{m^3}$	S21	This study
$K_{m,biomin}^{CP}$	half-saturation substrate P:C ratio for PO_4 biomineralization	0.0002	$\frac{mol\ P}{mol\ C}$	S21	This study
k_{ocl}	Occlusion coefficient of sorbed PO_4	3.86	$10^{-13} s^{-1}$	S22	Yang et al. (2014)
$k_{des,f}$	PO_4 fast desorption rate from P_{lab} to PO_4	0.014	h^{-1}	S23	Van der Zee et al. (1989)
k_{abs}	PO_4 (ab)sorption rate from P_{lab} to P_{sorb}	651.8519	$\frac{\mu mol}{kg\ soil\ s}$	S22	Yang et al. (2014)
k_{des}	PO_4 desorption rate from P_{sorb} to P_{lab}	0.000733	$\frac{mol}{kg\ soil\ s}$	S22	Yang et al. (2014)
S_{om}^{max}	PO_4 sorption capacity of organic matter	0.4	$\frac{mmolP}{kg\ OM}$	S25	Thum et al. (2019)
$S_{mineral}^{max}$	PO_4 sorption capacity of mineral soil	0.0387	$\frac{molP}{kg\ soil}$	S25	Thum et al. (2019)
$K_{S,om}$	half-saturation concentration for PO_4 adsorption to OM	0.045	$\frac{mmolP}{kg\ OM}$	S25	Thum et al. (2019)
$K_{S,mineral}$	half-saturation concentration for PO_4 adsorption to soil mineral	0.00225	$\frac{mmolP}{kg\ soil}$	S25	Thum et al. (2019)

Table S2. Parameters for sensitivity analysis

Parameter	Processes
All the values vary between 80% and 120% of the default values in Table S1	
k_{dom}^{ads}	OM sorption
k_{dom}^{des}	OM sorption
k_{res}^{ads}	OM sorption
k_{res}^{des}	OM sorption
$k_{des,f}$	Nutrient acquisition
$\chi_{mic}^{C:N}$	Microbial growth and decay
$\chi_{mic}^{N:P}$	Microbial growth and decay
mic_{nue}	Microbial growth and decay
mic_{pue}	Microbial growth and decay
mic_{cue}^{min}	Microbial growth and decay
$\eta_{C,wl\rightarrow poly}$	Litter partitioning and turnover
$\eta_{C,sol\rightarrow dom}$	Litter partitioning and turnover
τ_{mic}	Microbial growth and decay
$v_{max,upt}^{dom}$	Microbial growth and decay
$v_{max,depoly}^{poly}$	Depolymerisation
$v_{max,depoly}^{res}$	Depolymerisation
$\eta_{res\rightarrow dom}^{P}$	Microbial growth and decay
$\eta_{res\rightarrow dom}^{N}$	Microbial growth and decay
$v_{max,mic}^{nh_4}$	Nutrient acquisition
$v_{max,mic}^{no_3}$	Nutrient acquisition
$v_{max,mic}^{po_4}$	Nutrient acquisition
$k_{enz,mic}^{N}$	Nutrient acquisition
$k_{enz,mic}^{P}$	Nutrient acquisition
$k_{enz,root}^{N}$	Nutrient acquisition
$k_{enz,root}^{P}$	Nutrient acquisition
k_{weath}	Soil Pi cycle
k_{ocl}	Soil Pi cycle
$v_{max,biomin}$	Soil Pi cycle

References

Ahrens, B., Braakhekke, M. C., Guggenberger, G., Schrumpf, M., and Reichstein, M.: Contribution of sorption, DOC transport and microbial interactions to the 14C age of a soil organic carbon profile: Insights from a calibrated process model, Soil Biology and Biochemistry, 88, 390–402, https://doi.org/10.1016/j.soilbio.2015.06.008, http://dx.doi.org/10.1016/j.soilbio.2015.06.008, 2015.

Ahrens, B., Reichstein, M., Guggenberger, G., and Schrumpf, M.: Towards reconciling radiocarbon and carbon in soils: the importance of modelling organo-mineral associations, In prep.

Barrow, N. J.: The description of phosphate adsorption curves, Journal of Soil Science, 29, 447–462, 1978.

Bünemann, E. K., Augstburger, S., and Frossard, E.: Dominance of either physicochemical or biological phosphorus cycling processes in temperate forest soils of contrasting phosphate availability, Soil Biology and Biochemistry, 101, 85–95, https://doi.org/10.1016/j.soilbio.2016.07.005, 2016.

Davidson, E. A., Samanta, S., Caramori, S. S., and Savage, K.: The Dual Arrhenius and Michaelis-Menten kinetics model for decomposition of soil organic matter at hourly to seasonal time scales, Glob. Change Biol., 18, 371–384, 2012.

Kavka, M. and Polle, A.: Phosphate uptake kinetics and tissue-specific transporter expression profiles in poplar (Populus × canescens) at different phosphorus availabilities, BMC Plant Biology, 16, 206, https://doi.org/10.1186/s12870-016-0892-3, https://doi.org/10.1186/s12870-016-0892-3, 2016.

Koven, C. D., Riley, W. J., Subin, Z. M., Tang, J. Y., Torn, M. S., Collins, W. D., Bonan, G. B., Lawrence, D. M., and Swenson, S. C.: The effect of vertically resolved soil biogeochemistry and alternate soil C and N models on C dynamics of CLM4, Biogeosciences, 10, 7109–7131, 2013.

Kuzyakov, Y. and Xu, X.: Competition between roots and microorganisms for nitrogen: mechanisms and ecological relevance, New Phytologist, 198, 656–669, https://doi.org/doi:10.1111/nph.12235, https://nph.onlinelibrary.wiley.com/doi/abs/10.1111/nph.12235, 2013.

Lang, F., Krüger, J., Amelung, W., Willbold, S., Frossard, E., Bünemann, E. K., Bauhus, J., Nitschke, R., Kandeler, E., Marhan, S., Schulz, S., Bergkemper, F., Schloter, M., Luster, J., Guggisberg, F., Kaiser, K., Mikutta, R., Guggenberger, G., Polle, A., Pena, R., Prietzel, J., Rodionov, A., Talkner, U., Meesenburg, H., von Wilpert, K., Hölscher, A., Dietrich, H. P., and Chmara, I.: Soil phosphorus supply controls P nutrition strategies of beech forest ecosystems in Central Europe, Biogeochemistry, https://doi.org/10.1007/s10533-017-0375-0, 2017.

Manzoni, S., Porporato, A., and Schimel, J. P.: Soil heterogeneity in lumped mineralization–immobilization models, Soil Biology and Biochemistry, 40, 1137–1148, 2008.

Parton, W. J., Scurlock, J. M. O., Ojima, D. S., Gilmanov, T. G., Scholes, R. J., Schimmel, D. S., Kirchner, T., Menaut, J. C., Seastedt, T., Moya, E. G., Kamnalrut, A., and Kinyamario, J. I.: Observations and modelling of biomass and soil organic matter dynamics for the grassland biome worldwide, Global Biogeochemical Cycles, 7, 785–809, 1993.

Schimel, J. P. and Weintraub, M. N.: The implications of exoenzyme activity on microbial carbon and nitrogen limitation in soil: A theoretical model, Soil Biology and Biochemistry, 35, 549–563, https://doi.org/10.1016/S0038-0717(03)00015-4, http://linkinghub.elsevier.com/retrieve/pii/S0038071703000154, 2003.

Sinsabaugh, R. L., Turner, B. L., Talbot, J. M., Waring, B. G., Powers, J. S., Kuske, C. R., Moorhead, D. L., and Follstad Shah, J. J.: Stoichiometry of microbial carbon use efficiency in soils, Ecological Monographs, 86, 172–189, https://doi.org/10.1890/15-2110.1, http://dx.doi.org/10.1890/15-2110.1, 2016.

Tang, J. Y. and Riley, W. J.: A total quasi-steady-state formulation of substrate uptake kinetics in complex networks and an example application to microbial litter decomposition, Biogeosciences, 10, 8329–8351, https://doi.org/10.5194/bg-10-8329-2013, <GotoISI>://WOS:000329054600033, 2013.

Thum, T., Caldararu, S., Engel, J., Kern, M., Pallandt, M., Yu, L., and Zaehle, S.: A new terrestrial ecosystem model with coupled carbon, nitrogen, and phosphorus cycles (QUINCY v1.0; revision 1610), https://projects.bgc-jena.mpg.de/QUINCY/browser/project-A/tags/tag1, 2019.

Van der Zee, S., Leus, F., and Louer, M.: Prediction of phosphate transport in small columns with an approximate sorption kinetics model, Water Resources Research, 25, 1353–1365, 1989.

Wang, G., Post, W. M., Mayes, M. A., Frerichs, J. T., and Sindhu, J.: Parameter estimation for models of ligninolytic and cellulolytic enzyme kinetics, Soil Biology and Biochemistry, 48, 28–38, https://doi.org/https://doi.org/10.1016/j.soilbio.2012.01.011, http://www.sciencedirect.com/science/article/pii/S0038071712000247, 2012.

Wang, G., Post, W. M., and Mayes, M. A.: Development of microbial-enzyme-mediated decomposition model parameters through steady-state and dynamic analyses, Ecological Applications, 23, 255–272, https://doi.org/10.1890/12-0681.1, https://esajournals.onlinelibrary.wiley.com/doi/abs/10.1890/12-0681.1, 2013.

Wang, Y. P., Law, R. M., and Pak, B.: A global model of carbon, nitrogen and phosphorus cycles for the terrestrial biosphere, Biogeosciences, 7, 2261–2282, 2010.

White, M. A., Thornton, P. E., Running, S., and Nemani, R.: Parameterization and Sensitivity Analysis of the BIOME-BGC Terrestrial Ecosystem Model: Net Primary Production Controls, Earth Interactions, 4, 1–55, 2000.

Wutzler, T., Zaehle, S., Schrumpf, M., Ahrens, B., and Reichstein, M.: Adaptation of microbial resource allocation affects modelled long term soil organic matter and nutrient cycling, Soil Biology and Biochemistry, 115, 322–336, https://doi.org/https://doi.org/10.1016/j.soilbio.2017.08.031, http://www.sciencedirect.com/science/article/pii/S0038071717305680, 2017.

Yang, X., Thornton, P. E., Ricciuto, D. M., and Post, W. M.: The role of phosphorus dynamics in tropical forests – a modeling study using CLM-CNP, Biogeosciences, 11, 1667–1681, https://doi.org/10.5194/bg-11-1667-2014, https://www.biogeosciences.net/11/1667/2014/, 2014.

Zhu, Q., Riley, W. J., Tang, J., and Koven, C. D.: Multiple soil nutrient competition between plants, microbes, and mineral surfaces: model development, parameterization, and example applications in several tropical forests, Biogeosciences, 13, 341–363, https://doi.org/10.5194/bg-13-341-2016, 2016.

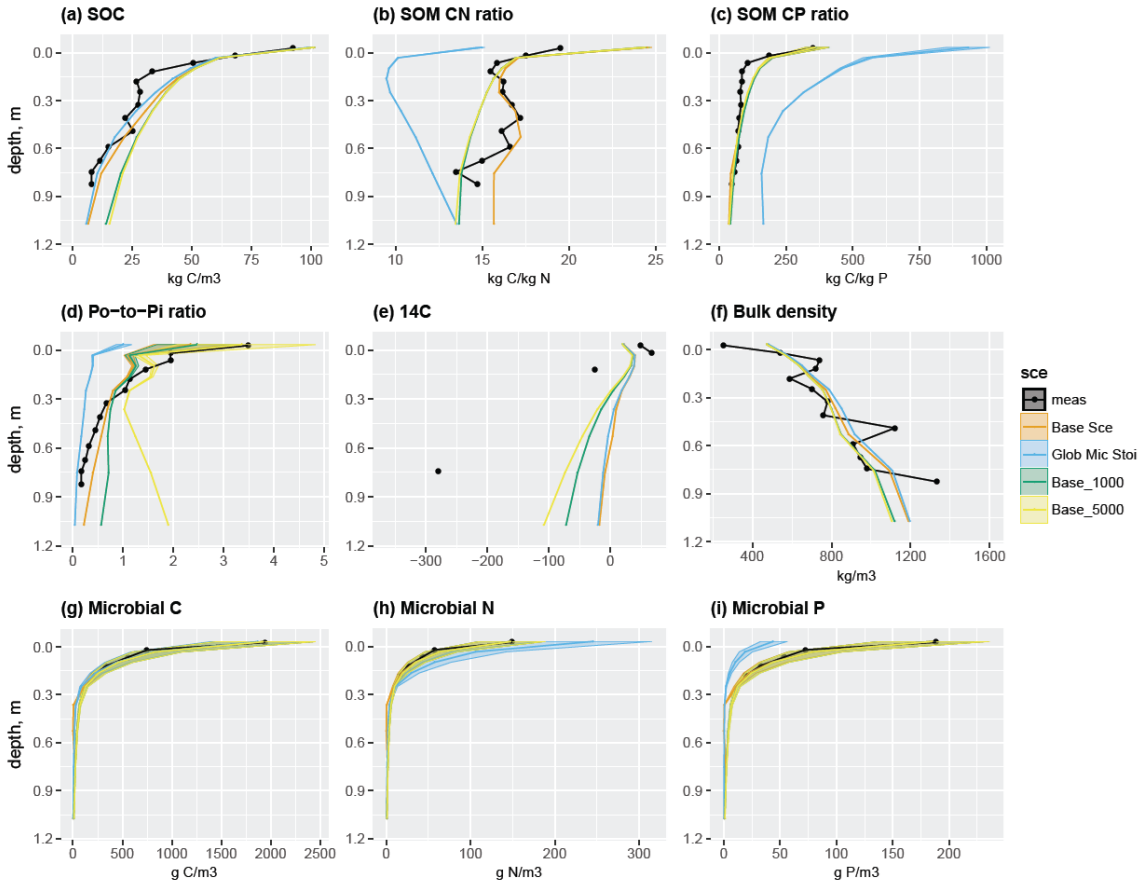

Figure S1. Simulated and observed (a) SOC content, (b) C:N ration in SOM, (c) C:P ratio in SOM, (d) organic P to inorganic P ratio in soil, microbial C, N, and P content ((e) to (g)), and (h) soil bulk density at the study site up to 1m soil depth. Black lines and dots: observations; Color lines and shades: simulated mean values and ranges of standard deviation by Base Scenario, the Global Microbial Stoichiometry (Glob. Mic. Stoi), and the extended base scenarios with simulation length of 1000 years (Base_1000) and 5000 years (Base_5000). The microbial C, N, and P are only measured in top 30cm soil. Simulated means and standard deviations are calculated using data of the last 10 years from the model experiments.

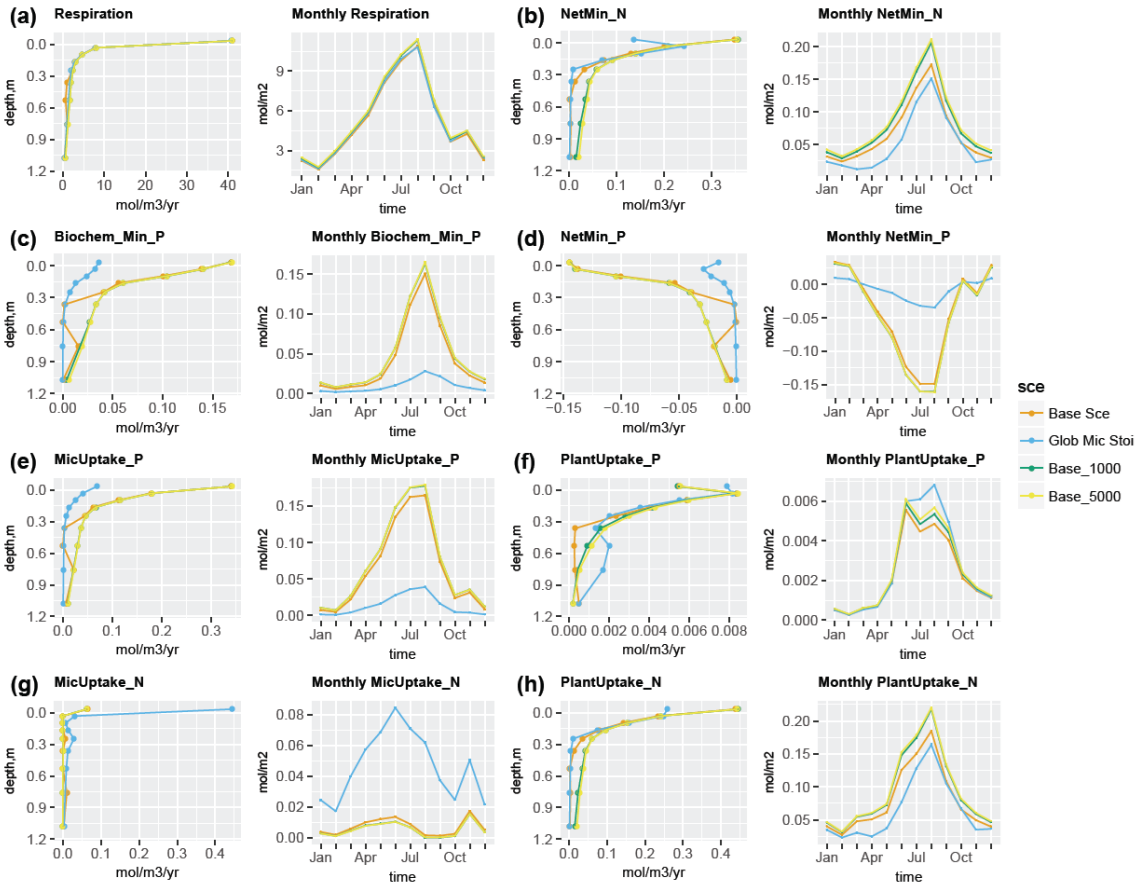

Figure S2. Simulated seasonal and vertical distribution of (a) respiration, (b) net N mineralisation, (c) biochemical P mineralisation, (d) net P mineralisation, (e) microbial inorganic P uptake, (f) plant P uptake, (g) microbial inorganic N uptake, and (h) plant N uptake at the study site up to 1m soil depth. Points represent the mean values and error bars represent the standard deviations, both calculated using data of the last 10 years from the model experiments.

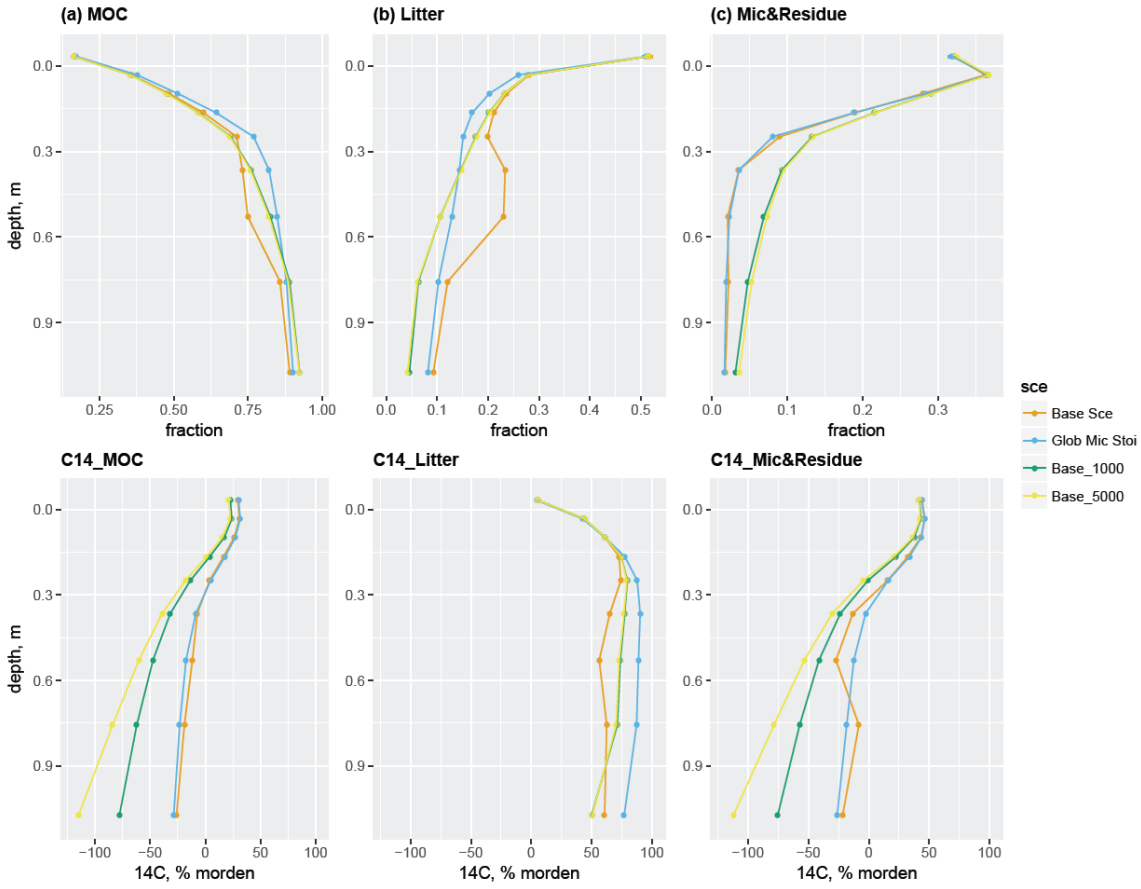

Figure S3. Simulated SOC fractions (upper panel) and their respective radiocarbon profiles (bottom panel) for up to 1m soil depth. Column (a): mineral-associated carbon (MOC), including adsorbed DOM and adsorbed microbial residue; Column (b): litter, including woody, polymeric and soluble litter; Column (c): live and dead microbes. Data points are derived from the last 10 years' data of the model experiments.

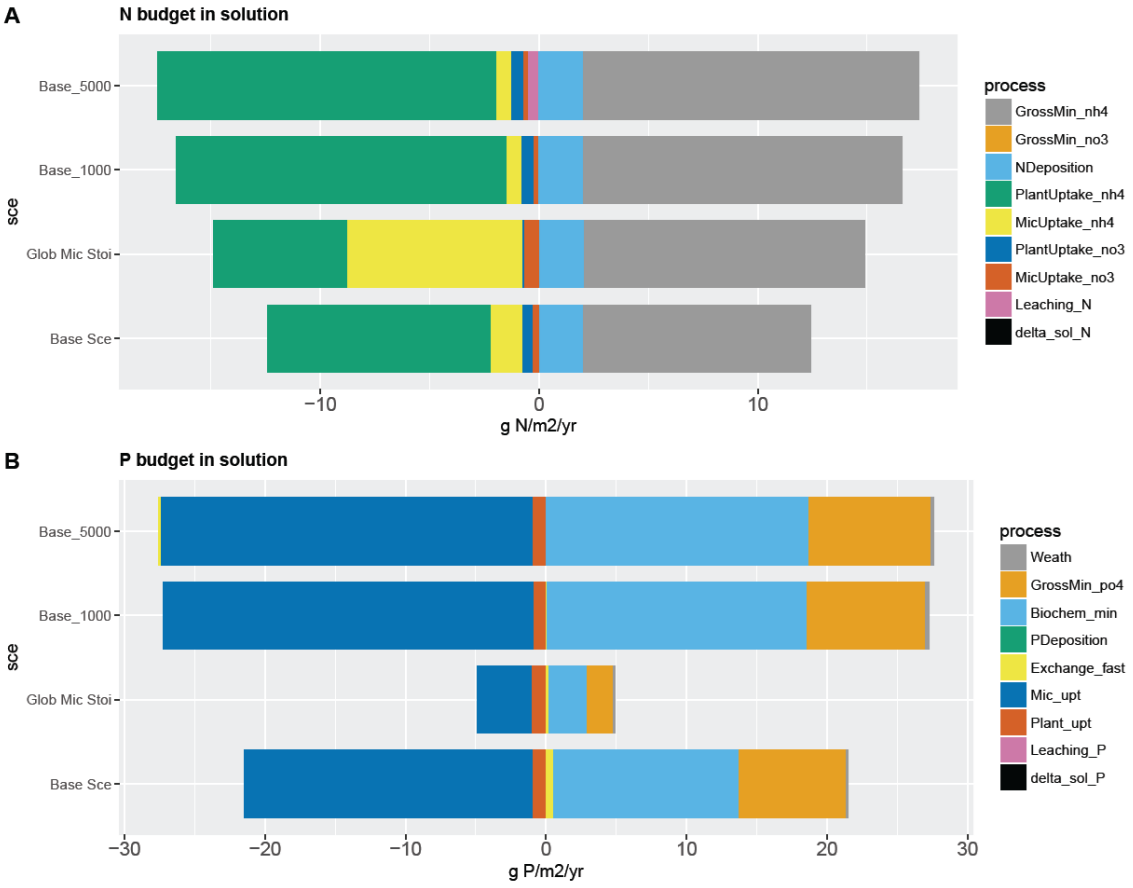

Figure S4. Simulated yearly budget of (A) nitrogen and (B) phosphorus in soil solution. In panel A, sourcing fluxes of N includes gross mineralisation of NH_4 and NO_3, N deposition; sinking fluxes of N includes plant and microbial uptake of NH_4, plant and microbial uptake of NO_3, N leaching (both inorganic and organic), and size change of soluble N ($delta\_sol\_N$). In panel B, sourcing fluxes of P includes weathering, gross mineralisation of PO_4, biochemical mineralisation of PO_4, P deposition; sinking fluxes of P includes adsorption ($Exchange\_fast$), microbial and plant uptake, P leaching (both inorganic and organic), and size change of soluble P ($delta\_sol\_P$). The budget are calculated using data of the full simulation from the model experiments.

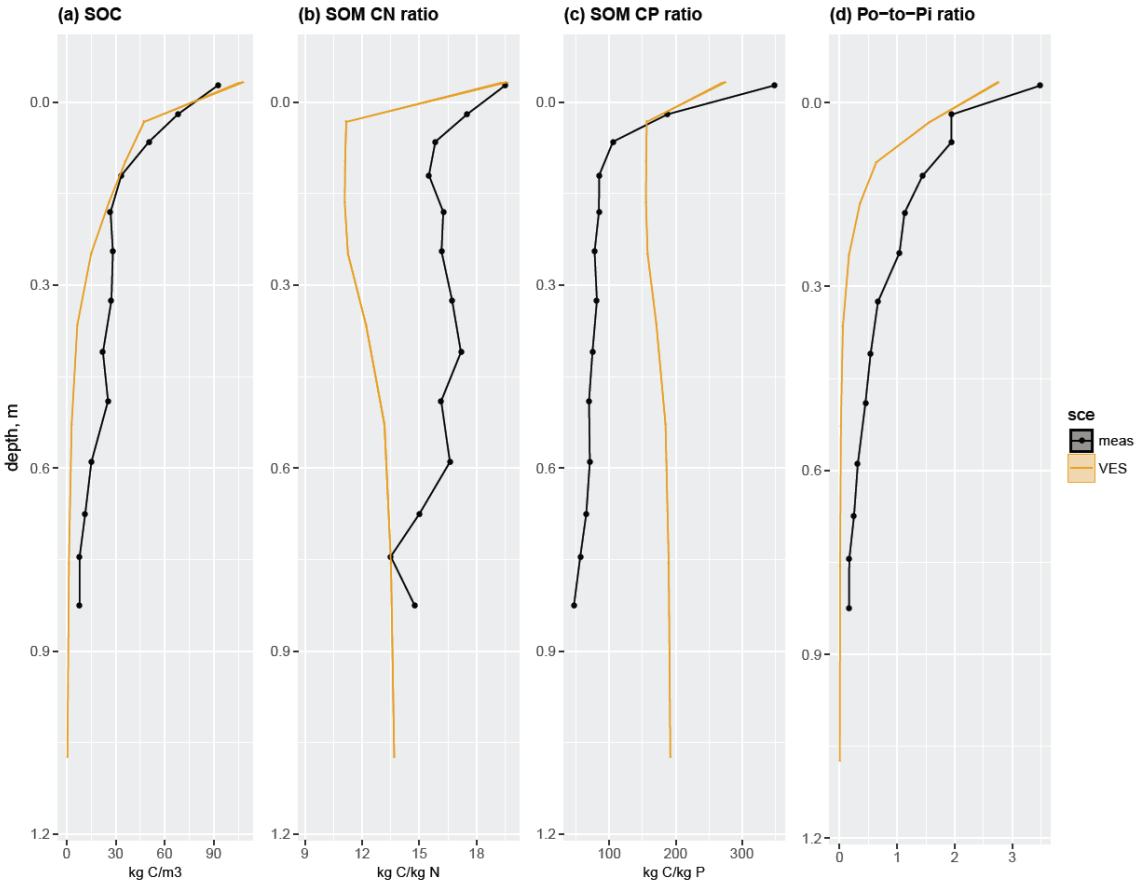

Figure S5. QUINCY simulated and observed (a) SOC content, (b) C:N ration in SOM, (c) C:P ratio in SOM, (d) organic P to inorganic P ratio in soil at the study site up to 1m soil depth. Black lines and dots: observations; Organe lines and shades: simulated mean values and ranges of standard deviation using QUINCY model(Thum et al., 2019). Simulated means and standard deviations are calculated using data of the last 10 years from the model experiments.